



Formation of Ti–Zr–Cu–Ni–Sn–Si bulk metallic glasses with good plasticity

Enhui Yin, Min Zhang, Shujie Pang, Xiangjin Zhao, Tao Zhang*

Key Laboratory of Aerospace Materials and Performance (Ministry of Education), School of Materials Science and Engineering, Beihang University, Beijing 100191, China

ARTICLE INFO

Article history:

Received 3 December 2009

Received in revised form 29 March 2010

Accepted 2 April 2010

Available online 9 April 2010

Keywords:

Amorphous materials

Rapid-solidification

Microstructure

Mechanical properties

ABSTRACT

Formation and mechanical properties of Ti–Zr–Cu–Ni–Sn–Si glassy alloys consisting of dissimilar and similar elements are studied. $\text{Ti}_{45.8}\text{Zr}_{6.2}\text{Cu}_{39.9}\text{Ni}_{5.1}\text{Sn}_2\text{Si}_1$ glassy alloy can be prepared in a bulk glassy rod form of 4 mm in diameter and exhibits strength of 2100 MPa and a plastic strain of ~5% prior to failure in compression. The plasticity of the $\text{Ti}_{45.8}\text{Zr}_{6.2}\text{Cu}_{39.9}\text{Ni}_{5.1}\text{Sn}_2\text{Si}_1$ bulk metallic glass is attributed to the deformation-induced nanocrystallization in the glassy matrix during compression.

© 2010 Elsevier B.V. All rights reserved.

1. Introduction

In the last decade, Ti-based bulk metallic glasses (BMGs) have gained significant interests in basic science and engineering aspects due to the combination of their high specific strength, large elastic limit and good corrosion resistance [1,2]. Several Ti-based BMGs have been developed in Ti(–Zr)–TM–M (TM = Cu, Ni and M = Si, Sn, B) alloy systems, such as Ti–Cu–Ni–B–Si–Sn [3], Ti–Zr–Ni–Cu–Sn [4], and Ti–Zr–Hf–Cu–Ni–Si [5], for which the critical diameters for glass formation were in the range from 1 to 5 mm by copper mold casting method. Ti-based BMGs with both high GFA and excellent deformability like Ti–Zr–Cu–Ni–Be [6] or Ti–Zr–Cu–Pd–Sn [7] have been reported. Exploring new Be or Pd-free Ti-based BMGs with high GFA and good plastic deformability is significant for the practical application of BMGs.

On the other hand, the effect of component elements on GFA of alloys has been studied extensively. It is generally recognized that the main constituent elements of the alloys with high GFA have significant difference in atomic size and negative heats of mixing. Recently, we found that the coexistence of dissimilar and similar elements can obviously improve the glass-forming ability. The superior glass formers [8,13], such as (La–Ce)–Al–(Co–Cu) BMGs (containing similar element pairs of La–Ce and Co–Cu in dissimilar element frameworks of RE–TM–Al) with critical diameter up to 32 mm [8,9], have been synthesized. Actually, the coexistence of dissimilar and similar elements can also be found in many previously reported superior glass formers, such as Pd–Cu–Ni–P [10],

Zr–Al–Ni–Cu [11], Fe–Co–Mo–Cr–C–B–Y [12]. The “coexistence criterion of dissimilar and similar elements” is effective in designing glassy alloy compositions with high GFA [8,13]. In this paper, we report the glass-forming ability, mechanical properties and thermal stability in (Ti–Zr)–(Cu–Ni)–(Sn–Si) alloy system consisting of dissimilar and similar elements. The origin of high GFA and plasticity of the Ti-based BMGs is discussed.

2. Experimental

Ti–Zr–Cu–Ni–Sn–Si alloy ingots were produced by arc-melting the mixture of pure elements with purities above 99.9% in a high-purity argon atmosphere. From the ingots, ribbons and cylindrical rods with different diameters were prepared by melt spinning and copper mold casting, respectively. The structure of the specimens was examined by X-ray diffraction (XRD) using $\text{Cu K}\alpha$ radiation and transmission electron microscopy (TEM). The samples for TEM observation were prepared by electrochemical polishing with a solution of 4% HClO_4 and 96% $\text{C}_2\text{H}_5\text{OH}$ at 243 K. Thermal stability of the glassy samples was evaluated by differential scanning calorimeter (DSC) at a heating rate of 0.33 K/s. Compression tests for the BMGs were carried out by employing SANS testing machine at a strain rate of $2.1 \times 10^{-4} \text{ s}^{-1}$. The compression samples were 2 mm in diameter and 4 mm in length. The deformed specimens were observed by scanning electron microscope (SEM).

3. Results and discussion

A series of Ti-based alloys (I–VI) are designed in the present work, as listed in Table 1. XRD patterns of the as-cast alloy samples with different diameters are shown in Fig. 1. It can be seen that the patterns for the alloy rods consist of only broad diffraction halos without any sharp Bragg peak, except for the $\text{Ti}_{45.8}\text{Zr}_{6.2}\text{Cu}_{39.9}\text{Ni}_{5.1}\text{Sn}_2\text{Si}_1$, which is partially nanocrystallized specimen. Apparently, a small amount of Sn addition to the Ti–Zr–Cu–Ni system is effective on improving the GFA. The further minor addition of Si into the Ti–Zr–Cu–Ni–Sn resulted in a $\text{Ti}_{45.8}\text{Zr}_{6.2}\text{Cu}_{39.9}\text{Ni}_{5.1}\text{Sn}_2\text{Si}_1$ alloy with the highest GFA

* Corresponding author. Tel.: +86 10 82314869; fax: +86 10 82314869.
E-mail address: zhangtao@buaa.edu.cn (T. Zhang).

Table 1
Thermal properties and critical diameter (d_c) of Ti-based BMGs.

Alloy	Composition (at.%)	T_g /K	T_x /K	ΔT_x /K	d_c /mm
I	Ti ₄₅ Zr ₅ Cu ₄₅ Ni ₅	660	695	35	<2
II	Ti _{45.2} Zr _{7.2} Cu _{40.5} Ni _{5.1} Sn ₂	676	714	38	3
III	Ti _{44.2} Zr _{8.2} Cu _{40.5} Ni _{5.1} Sn ₂	664	706	32	3
IV	Ti _{43.2} Zr _{9.2} Cu _{40.5} Ni _{5.1} Sn ₂	680	716	36	3
V	Ti _{45.8} Zr _{6.2} Cu _{39.9} Ni _{5.1} Sn ₂ Si ₁	670	711	35	4
VI	Ti _{45.4} Zr _{6.1} Cu _{39.5} Ni ₅ Sn ₂ Si ₂	668	720	52	2

among the present alloys, for which the critical diameter is up to 4 mm.

DSC curves of the Ti-based rods with their critical diameters are shown in Fig. 2. The thermal properties associated with glass transition temperature T_g , onset crystallization temperature T_x and supercooled liquid region ΔT_x ($\Delta T_x = T_x - T_g$) are summarized in Table 1. The glassy Ti_{45.8}Zr_{6.2}Cu_{39.9}Ni_{5.1}Sn₂Si₁ rod with a diameter of 4 mm exhibited the same T_g , T_x and crystallization heat release as those for the as-spun ribbon, further confirming the glassy structure of the alloy rods.

Previous reports have shown that GFA can be significantly improved when the similar element substitution of Ti with Zr or Cu with Ni was applied in the binary Ti₅₀Cu₅₀ alloy [14,15]. Both Ti–Cu–Ni [14] with critical diameter of 2 mm and Ti–Zr–Cu–Ni BMG [15] with diameter of at least 3 mm have been successfully fabricated by copper mold casting. For the Ti–Zr–Cu–Ni–Sn–Si alloy, there is large negative heat of mixing between Ti–Sn, Zr–Sn, Ti–Si, Zr–Si and Ni–Si [16] and strong chemical short-range order is expected, which may stabilize the liquid and reduce the atomic mobility that mediates crystallization. On the other hand, the decrease of the Gibbs free energy (ΔG) caused by

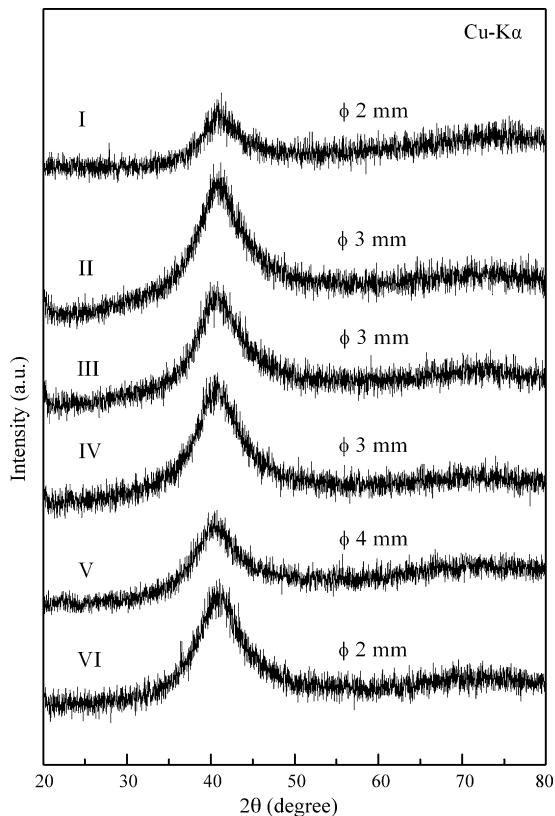


Fig. 1. XRD patterns from the as-cast rods with different diameters for the present alloys.

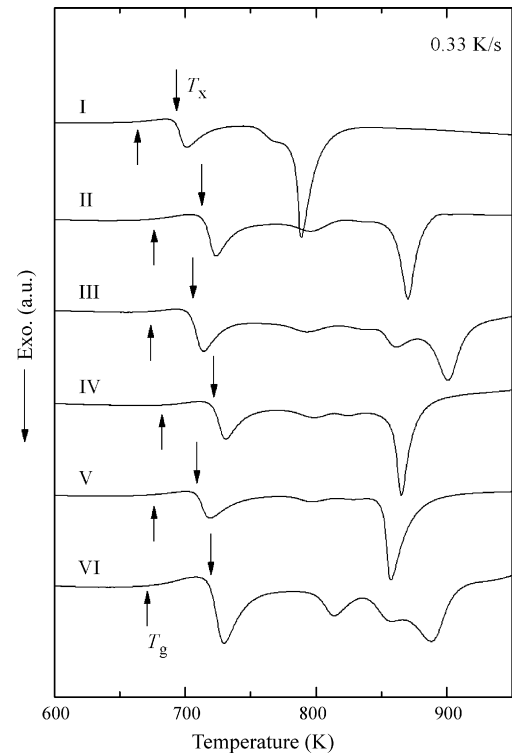


Fig. 2. DSC curves of the present alloy rods with critical diameters at a heating rate of 0.33 K/s.

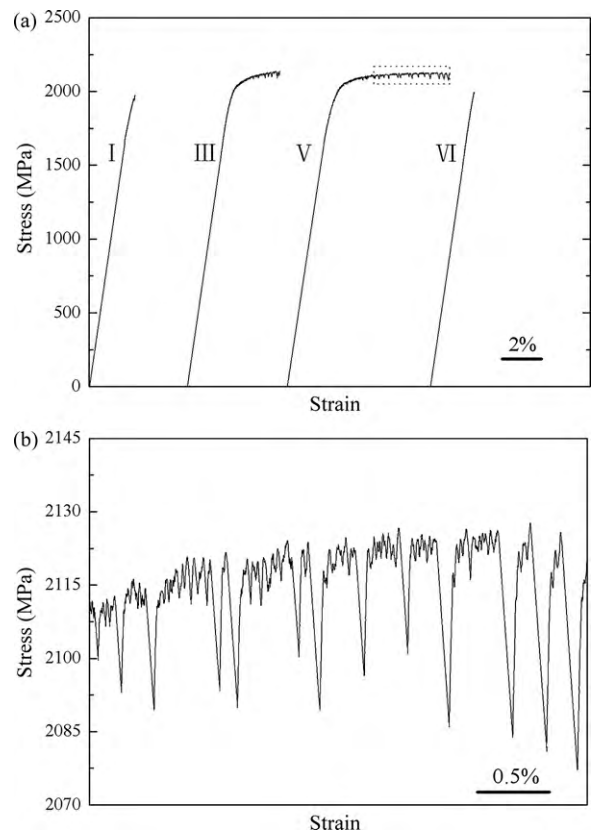


Fig. 3. (a) Compression stress–strain curves of four monolithic BMGs, including Ti₄₅Zr₅Cu₄₅Ni₅, Ti_{44.2}Zr_{8.2}Cu_{40.5}Ni_{5.1}Sn₂, Ti_{45.8}Zr_{6.2}Cu_{39.9}Ni_{5.1}Sn₂Si₁ and Ti_{45.4}Zr_{6.1}Cu_{39.5}Ni₅Sn₂Si₂. (b) The amplified curve of Ti_{45.8}Zr_{6.2}Cu_{39.9}Ni_{5.1}Sn₂Si₁ alloy in the image (a) shows a serrated flow.

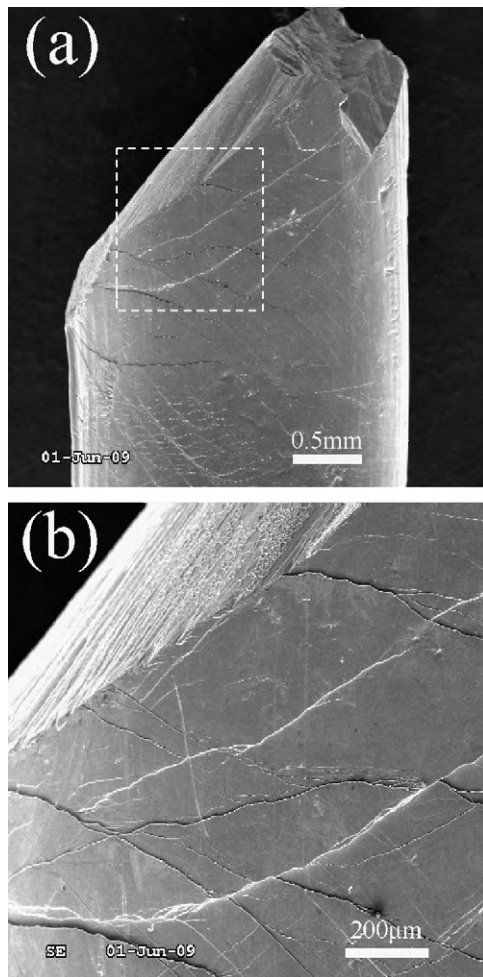


Fig. 4. (a) SEM image of surface of the deformed $\text{Ti}_{45.8}\text{Zr}_{6.2}\text{Cu}_{39.9}\text{Ni}_{5.1}\text{Sn}_2\text{Si}_1$ rod. (b) The enlarged image of the marked area in (a).

the configurational entropy, due to the coexistence of similar element pairs like Ti–Zr and Cu–Ni which have heat of mixing close to 0, is beneficial to the further enhancement of GFA [8].

Fig. 3(a) shows the compressive stress–strain curves of the I, III, V and VI BMGs. The four glassy alloys exhibit elastic strain of about 2% and fracture strength up to 2000 MPa. The plasticity of the glassy alloys is strongly influenced by the contents of Sn and Si elements. For $\text{Ti}_{45}\text{Zr}_5\text{Cu}_{45}\text{Ni}_5$ and $\text{Ti}_{45.4}\text{Zr}_{6.1}\text{Cu}_{39.5}\text{Ni}_5\text{Sn}_2\text{Si}_2$ alloys, neither yielding and nor plastic strain is observed in the stress–strain curves. However, $\text{Ti}_{44.2}\text{Zr}_{8.2}\text{Cu}_{40.5}\text{Ni}_{5.1}\text{Sn}_2$ and $\text{Ti}_{45.8}\text{Zr}_{6.2}\text{Cu}_{39.9}\text{Ni}_{5.1}\text{Sn}_2\text{Si}_1$ alloys show the plastic strain of 3% and 5%, respectively. The marked part of the stress–strain curve of the $\text{Ti}_{45.8}\text{Zr}_{6.2}\text{Cu}_{39.9}\text{Ni}_{5.1}\text{Sn}_2\text{Si}_1$ glassy alloy in Fig. 3(a) is amplified in Fig. 3(b), which demonstrates that plastic deformation proceeds mainly by numerous serrations. The serrations are generally small (~ 8 MPa) with a few large ones (~ 50 MPa).

Multiple shear bands can be observed on the lateral surface of fracture samples, as denoted in Fig. 4(a). The shear bands have a pronounced tendency to branch as they propagate through the specimens and branching can distribute the plastic strains associated with main shear band. Individual shear bands observed on the surface of the deformed samples are not associated with stress serrations that depend on the temperature and strain rate [17,18]. Some cracks in the vicinity of the fracture surface are observed on the lateral surface, as illustrated in Fig. 4(b). Shear bands can initiate

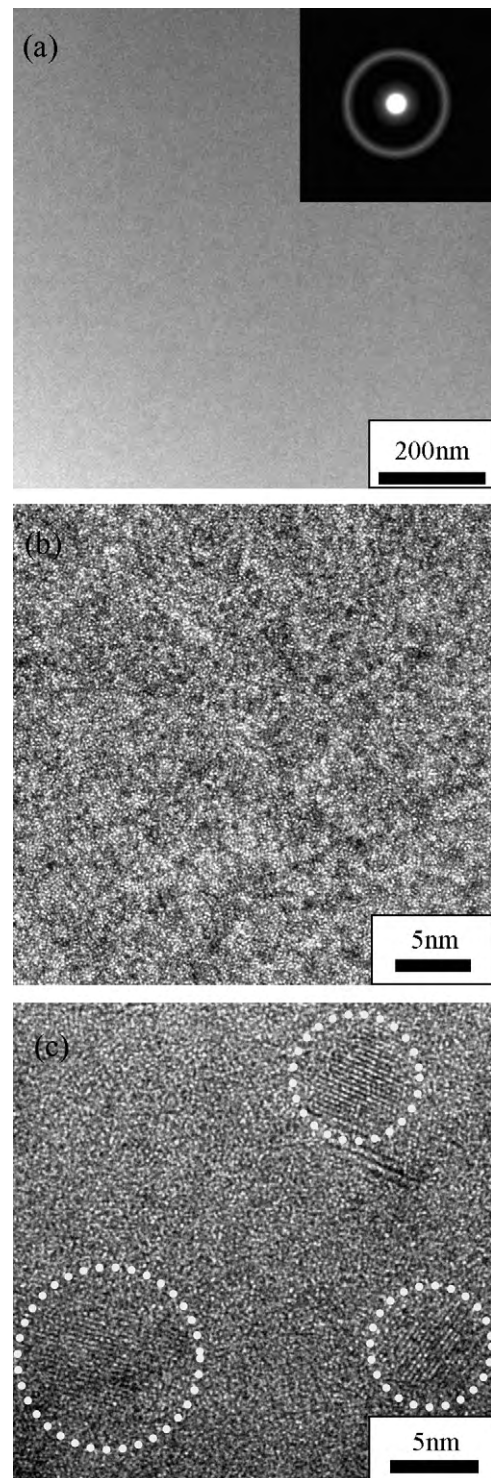


Fig. 5. (a) Bright field image with SAD pattern inserted. (b) The HRTEM image of the $\text{Ti}_{45.8}\text{Zr}_{6.2}\text{Cu}_{39.9}\text{Ni}_{5.1}\text{Sn}_2\text{Si}_1$ glassy rod with a diameter of 2 mm in as-cast state. (c) The HRTEM image of the rod sample after the compressive test at 298 K.

cracks, which will cause the macroscopic fracture [19]. Therefore, each large serration shown in Fig. 3(b) might be corresponding to the formation of a crack that could be leading to a remarkable stress drop.

The glassy structure for the as-cast $\text{Ti}_{45.8}\text{Zr}_{6.2}\text{Cu}_{39.9}\text{Ni}_{5.1}\text{Sn}_2\text{Si}_1$ rod of 2 mm in diameter is confirmed by the TEM and HRTEM observations, as shown in Fig. 5(a) and (b). However, the sam-

ple after the compressive test exhibits that crystalline particles of about 5 nm in size are randomly distributed in the amorphous matrix, as indicated in Fig. 5(c). Glassy alloys tend to transform into more stable crystalline phases with supply of thermal energy or after plastic deformation [20,21]. Under compressive stress, the precipitation of nanocrystallites along shear bands [22,23] may result from high temperatures caused by the energy dissipation of shear deformation [17,24]. On the other hand, the $\text{Ti}_{45.8}\text{Zr}_{6.2}\text{Cu}_{39.9}\text{Ni}_{5.1}\text{Sn}_2\text{Si}_1$ BMG has a very narrow supercooled liquid region of 35 K, indicating low stability of the supercooled liquid of this glassy alloy and easier precipitation of crystallites in the supercooled liquid state induced by localized temperature rising upon shear deformation. Therefore, nucleation and growth of crystallites may occur in the severely deformed glassy alloy. By the precipitation of the nanocrystalline particles, the propagation of corresponding shear band may be suppressed by the disappearance of the localized viscous flow [21,25]. Then, new shear bands could be initiated to accommodate the applied strain and therefore the high density of shear bands was formed, which may lead to the distinct plasticity of the $\text{Ti}_{45.8}\text{Zr}_{6.2}\text{Cu}_{39.9}\text{Ni}_{5.1}\text{Sn}_2\text{Si}_1$ glassy alloy.

4. Conclusions

The (Ti–Zr)–(Cu–Ni)–(Sn–Si) glassy alloys consisting of dissimilar and similar elements with high glass-forming ability and good plastic deformability in compression are synthesized by copper mold casting. For $\text{Ti}_{45.8}\text{Zr}_{6.2}\text{Cu}_{39.9}\text{Ni}_{5.1}\text{Sn}_2\text{Si}_1$ BMG, the critical diameter is 4 mm and plastic strain up to 5% and fracture strength of 2100 MPa in compression were achieved. Nanocrystalline particles precipitated in the glassy matrix for the fractured glassy rod exhibiting distinct plastic strain. The plasticity of $\text{Ti}_{45.8}\text{Zr}_{6.2}\text{Cu}_{39.9}\text{Ni}_{5.1}\text{Sn}_2\text{Si}_1$ glassy alloy was ascribed to the in situ nanocrystallization induced by deformation.

Acknowledgements

This work was financially supported by the National Basic Research Program of China (2007CB613900), the National Nature Science Foundation of China (Grant Nos. 50631010, 50771005 and 50771006) and Program for NCET (NCET-07-0041).

References

- [1] H.S. Chen, Rep. Prog. Phys. 43 (1980) 353–432.
- [2] A. Inoue, Acta Mater. 48 (2000) 279–306.
- [3] T. Zhang, A. Inoue, Mater. Sci. Eng. A 304–306 (2001) 771–774.
- [4] T. Zhang, A. Inoue, Mater. Trans. JIM 39 (1998) 1001–1006.
- [5] C.L. Ma, H. Soejima, S. Ishihara, K. Amiya, N. Nishiyama, A. Inoue, Mater. Trans. JIM 45 (2004) 3223–3227.
- [6] F.Q. Guo, H.J. Wang, S.J. Poon, G.J. Shiflet, Appl. Phys. Lett. 86 (2005) 091907.
- [7] S.L. Zhu, X.M. Wang, A. Inoue, Intermetallics 16 (2008) 1031–1035.
- [8] R. Li, S.J. Pang, C.L. Ma, T. Zhang, Acta Mater. 55 (2007) 3719–3726.
- [9] R. Li, F.J. Liu, S. Pang, C.L. Ma, T. Zhang, Mater. Trans. 48 (2007) 1680–1683.
- [10] A. Inoue, N. Nishiyama, Mater. Sci. Eng. A 226–228 (1997) 401–405.
- [11] T. Zhang, A. Inoue, T. Masumoto, Mater. Trans. JIM 32 (1991) 1005–1010.
- [12] J. Shen, Q.J. Chen, J.F. Sun, H.B. Fan, G. Wang, Appl. Phys. Lett. 86 (2005) 151907.
- [13] L.C. Zhuo, S.J. Pang, H. Wang, T. Zhang, Chin. Phys. Lett. 26 (2009) 066402.
- [14] X.F. Wu, Z.Y. Suo, Y. Si, L.K. Meng, K.Q. Qiu, J. Alloys Compd. 452 (2008) 268–272.
- [15] H. Men, S.J. Pang, A. Inoue, T. Zhang, Mater. Trans. JIM 46 (2005) 2218–2220.
- [16] F.R. de Boer, R. Boom, W.C.M. Mattens, A.R. Miedema, A.K. Niessen, Cohesion in Metals, North-Holland, Amsterdam, 1989, p. 103.
- [17] K. Georgarakis, M. Aljerf, Y. Li, A. LeMoulec, F. Charlot, A.R. Yavari, K. Chornokhvostenko, E. Tabachnikova, G.A. Evangelakis, D.B. Miracle, A.L. Greer, T. Zhang, Appl. Phys. Lett. 93 (2008) 031907.
- [18] W.H. Jiang, F. Jiang, F.X. Liu, H. Choo, P.K. Liaw, K.Q. Qiu, Appl. Phys. Lett. 89 (2006) 261909.
- [19] A.V. Sergueeva, N.A. Mara, J.D. Kuntz, D.J. Branagan, A.K. Mukherjee, Mater. Sci. Eng. A 383 (2004) 219–223.
- [20] Y.X. Zhuang, J.Z. Jiang, T.J. Zhou, H. Rasmussen, L. Gerward, Appl. Phys. Lett. 77 (2000) 4133–4135.
- [21] H. Men, T. Zhang, Mater. Trans. JIM 46 (2005) 2545–2547.
- [22] K. Hajlaoui, A.R. Yavari, B. Doisneau, A. LeMoulec, W.J. Botta, G. Vaughan, A.L. Greer, A. Inoue, W. Zhang, Å. Kvick, Scripta Mater. 54 (2004) 1829–1834.
- [23] K. Hajlaoui, B. Doisneau, A.R. Yavari, W.J. Botta, W. Zhang, G. Vaughan, A. Kvick, A. Inoue, A.L. Greer, Mater. Sci. Eng. A 449–451 (2007) 105–110.
- [24] J.J. Lewandowski, A.L. Greer, Nat. Mater. 5 (2006) 15–18.
- [25] T. Zhang, H. Men, J. Alloys Compd. 434–435 (2007) 10–12.